Int J Adv Manuf Technol (2010) 51:1–14
DOI 10.1007/s00170-010-2620-8

ORIGINAL ARTICLE

A combined FEA and design of experiments approach for the design and analysis of warm forming of aluminum sheet alloys

Hong Seok Kim

Received: 26 November 2009 / Accepted: 8 March 2010 / Published online: 31 March 2010

Abstract This paper presents a methodology to effectively determine the optimal process parameters for warm forming of lightweight materials using finite element analysis (FEA) and design of experiments (DOE). The accuracy and effectiveness of FEA are verified through comparisons of the achievable part depth values and forming limits predicted from FEA with those from experimental measurements in a wide range of warm-forming conditions. A DOE approach along with FEA is proposed to offer rapid and relatively accurate design of warm-forming process, especially for large parts that require 3D FEA. In addition, strain distributions on the formed part are obtained under a variety of process conditions to gain a better understanding of the warm-forming mechanisms and further investigate the effects of forming temperature, friction condition, forming speed, and blank holding pressure on forming performance. Results of this study reveal that much-improved formability can be efficiently gained with a well-controlled warm-forming parameters.

Keywords Warm forming · Lightweight materials · Finite element analysis · Design of Experiments · Taguchi methodology

1 Introduction

In order to protect the environment, ensure a healthy society, and preserve the natural resources for the next generations, sustainable development policies have been discussed at various forums [1, 2]. Weight reduction of the vehicles (aircraft, automotive, ship, and trains) is one of such enablers and can be realized by the development and design of novel manufacturing processes that can convert lightweight materials such as aluminum and magnesium alloys into functional structures in a cost-effective manner. Forming technologies such as net-shape forging and stamping offer a viable means to achieve it since forming is well known for its high production rate, minimized material waste, near-net-shapes, excellent mechanical properties, and close tolerances[3–5]. Lightweight material content in the ground vehicles, however, is mostly limited to few cast and hot forged underbody parts since the inferior formability of lightweight materials makes it more difficult and expensive to use them in mass production of structural and body parts.

A number of studies have shown the potential of warm-forming process to achieve increased formability of lightweight materials. It was reported that at elevated temperature level (200-350°C) aluminum-magnesium alloys achieved an elongation up to 300% [6]. A significant increase in formability with 5XXX and 6XXX series of aluminum and AZ31, AZ61 magnesium alloys was also verified [7–9]. Some early experimental studies confirmed a strong effect of both strain rate hardening and strain hardening on formability and the improvement of formability at elevated temperatures were mainly attributed to the enhanced strain rate sensitivity with increasing temperature [10, 11]. Various attempts on warm forming of lightweight materials, however, have not gone beyond lab-scale experiments on simple cups [12, 13] and only few number of prototype trials in the industry [14, 15] because of various underlying unknowns including the complex interaction between the temperature and mechanical behavior of materials, complex friction conditions and suitable lubricants, and favorable process conditions and parameters operating window.

H. S. Kim (✉)
Department of Mechanical Engineering,
Seoul National University of Technology,
172 Gongneung 2-dong, Nowon-gu,
Seoul 139-743, Korea
e-mail: hongseok@snut.ac.kr

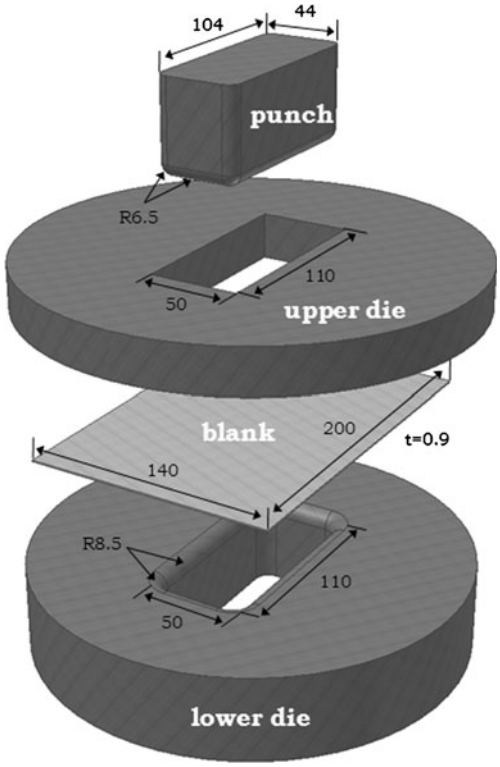

Fig. 1 FE model for rectangular cup part forming

Recent progresses in finite element analysis (FEA) enabled a remarkable development in metal forming and led to shorter lead time and cost saving. Takuda et al. [16] developed a numerical model using the rigid plastic and the heat conduction finite element methods to analyze the deformation behavior of an aluminum alloy sheet (Al 5182-O) at elevated temperature. Palaniswamy et al. [17] demonstrated the feasibility of FEA tools (2D and 3D) in predicting material flow and thickness variation based on experimental study by Droder [18]. Many researchers also used FEA in combination with different optimization techniques to improve forming performance and develop re-usable guidelines [19]. However, since most of the existing optimization techniques such as sensitivity analysis [20], neural network [21], and genetic algorithm [22] are based on the iterative search algorithm, a large number of simulations are required and their computational cost is still very high, especially for industrial-size complex parts. Therefore, existing iteration-based optimization approaches have a limitation in the practical application for the design and control of warm-forming process that could enable its rapid and wider application to industrial production opportunities.

This paper presents an alternative method to effectively determine the proper process condition for warm forming of an aluminum alloy. Based on the accuracy and reliability of non-isothermal FEA proved in the preliminary study of the author [23], we implemented Taguchi methodology as one form of DOE to identify the optimal process parameters which maximize the formability in a rectangular cup-forming case. This combined FEA and DOE approach provided a reasonably accurate and cost-effective mean to reach the optimal design point in a short computational time. In addition, the effects of process parameters such as forming temperature, friction, forming speed, and blank-holding pressure on forming performance were investigated by constructing and comparing thickness stress distributions on the formed part in a wide range of warm-forming conditions.

2 Finite element model

In order to analyze the warm forming of a rectangular cup part, a thermo-mechanically coupled finite element (FE)

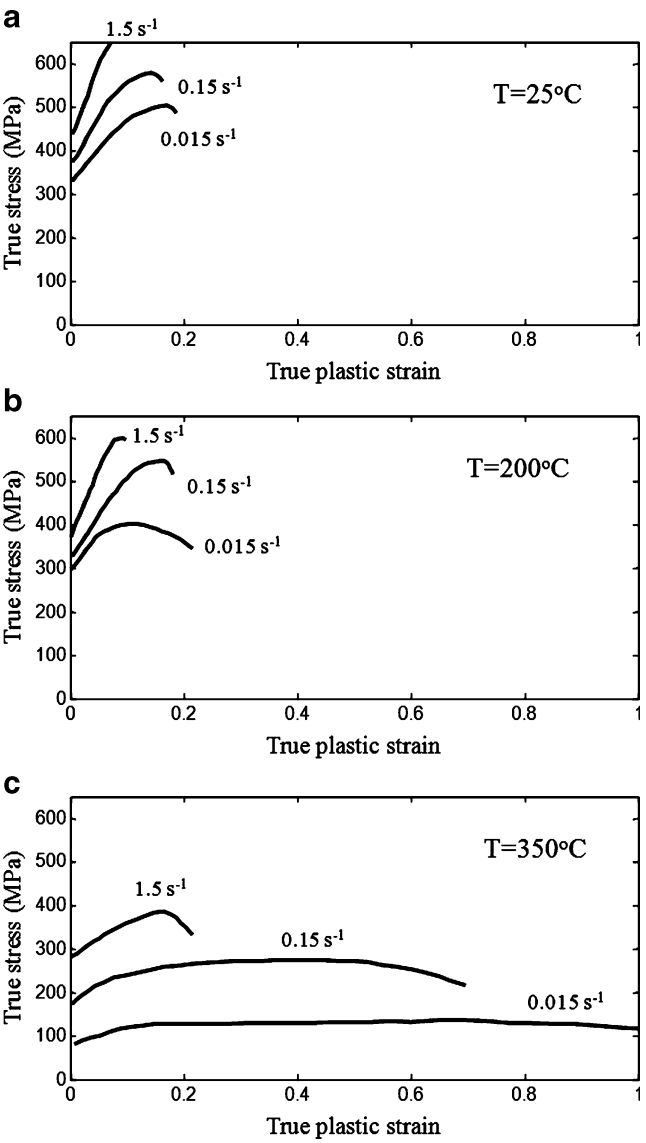

Fig. 2 Stress-stain relationship of Al5182+Mn at three different temperatures and strain rates [10]. **a** T=25°C, **b** T=200°C, **c** T=350°C

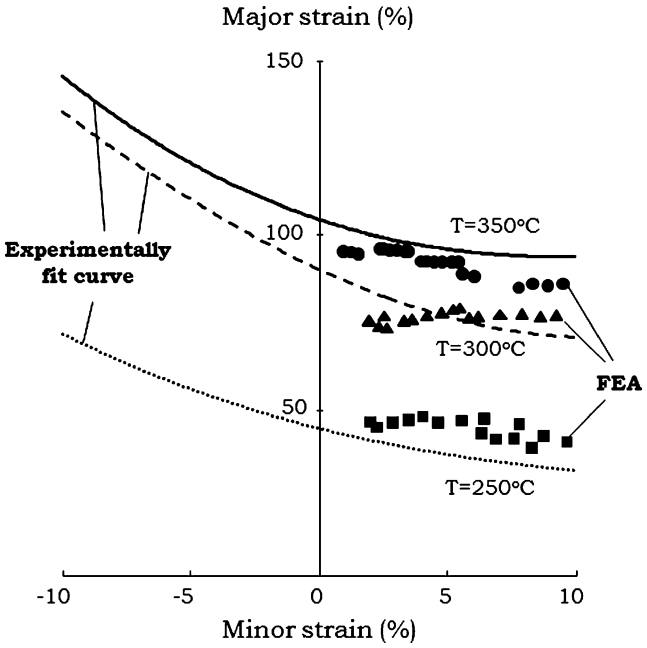

Fig. 3 Comparison of FEA prediction with experimental findings [23]. Effect of forming temperature on forming limit diagram

model was developed. Commercially available FEA software, ABAQUS/EXPLICT was used and the detailed geometric features were illustrated in Fig. 1. An aluminum alloy of Al 5182+Mn was used for the material. As shown in Fig. 2, stress-strain behavior of the Al 5182+Mn was measured in tensile tests at three different temperatures (25, 200, and 350°C) and strain rates (0.015, 0.15, and 1.5 s^{-1}) [10] and was used in simulation by fitting the curves up to the maximum tensile strength. For simplicity, tooling distortion due to temperature changes was ignored and uniform temperature distribution was directly assigned on the tooling surfaces to describe warm-forming conditions. The heat transfer effect, however, was included at the interface between the blank and the tooling elements. The blank temperature was initially 25°C, and heated in the tooling by conduction heat transfer from the dies and punch. The contact heat transfer coefficient of 1,400 W/m^2K was obtained from Takuda et al. [16] for similar condition, and assumed to be uniform regardless of the temperature and pressure at the interface. The heat loss of the blank by natural convection was also included. The heat transfer coefficients calculated at different temperature levels were 14.7, 14, and 12.8 W/m^2K at 400°C, 300°C, and 200°C, respectively. Regarding the boundary conditions, displacements of all lower die nodes were constrained according to the assumption of a rigid body, and the nodes of the punch and the upper die were allowed to

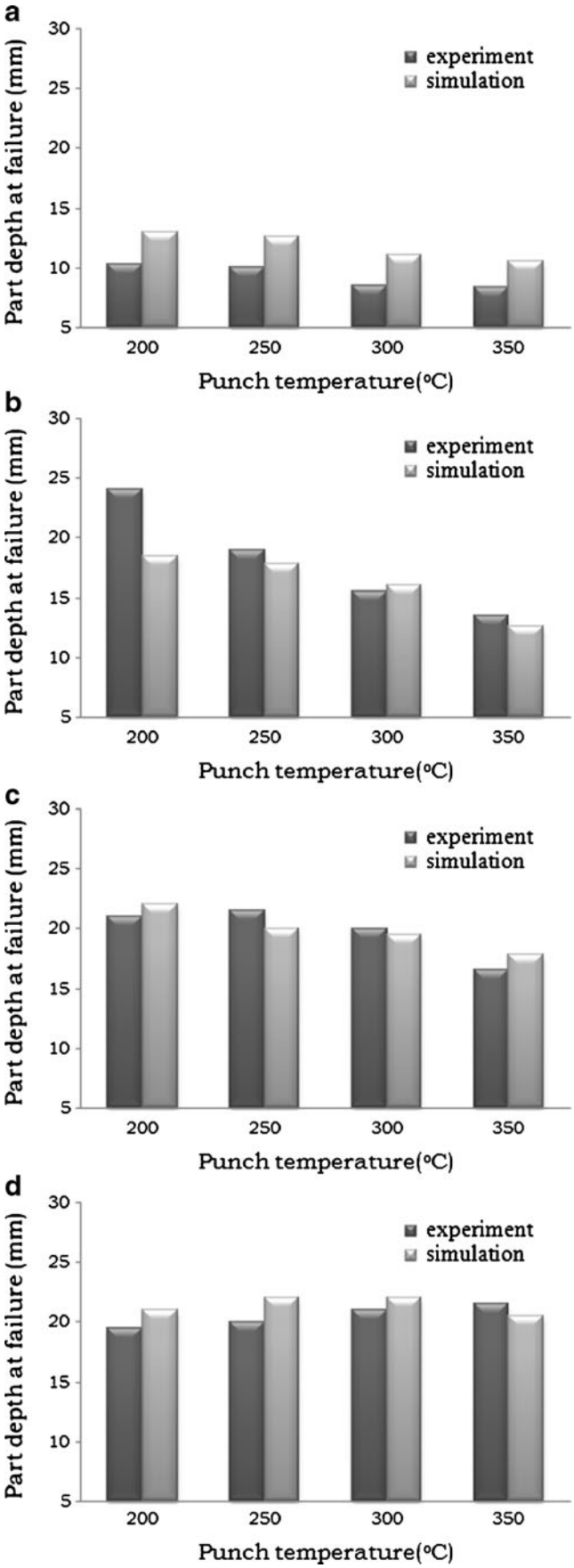

Fig. 4 Comparison of FEA predictions with experimental findings [23]. Effect of die and punch temperature on part depth. **a** T_{die}=200°C, **b** T_{die}=250°C, **c** T_{die}=300°C, **d** T_{die}=350°C

Table 1 Levels of the variables

Symbol	Controllable factors	Level		
		1	2	3
A	Temperature of lower die (°C)	25	250	350
B	Temperature of punch (°C)	25	250	350
C	Temperature of upper die (°C)	25	250	350
D	Friction coefficient between die and blank	0.05	0.1	0.2
E	Friction coefficient between punch and blank	0.05	0.01	0.2
F	Punch speed (mm/s)	5	10	20
G	Blank holding pressure (MPa)	1	2	4

move only in the vertical direction. Uniform blank holding pressure was applied to the top surface of the upper die and the punch was moved down at a fixed speed to form a rectangular cup part. 3D brick elements, C3D8RT, having both temperature and displacement degrees of freedom were used to describe the model, and five layers of this element were used through the thickness of the blank to allow for the prediction of nonlinear bending and frictional shear strain. The onset of localized necking was determined when the local thickness ratio between elements dropped below 0.94 based on the previous experimental study of the author [23].

The accuracy and reliability of the FE model were validated from the comparison with the experiments [23]. As illustrated in Fig. 3, predicted forming limit from the

Table 2 L_{27} orthogonal array with design factors and interactions assigned

Trial no.	Column numbers												
	1 A	2 B	3 A×B	4 A×B	5 C	6 A×C	7 A×C	8 B×C	9 D	10 E	11 B×C	12 F	13 G
1	1	1	1	1	1	1	1	1	1	1	1	1	1
2	1	1	1	1	2	2	2	2	2	2	2	2	2
3	1	1	1	1	3	3	3	3	3	3	3	3	3
4	1	2	2	2	1	1	1	2	2	2	3	3	3
5	1	2	2	2	2	2	2	3	3	3	1	1	1
6	1	2	2	2	3	3	3	1	1	1	2	2	2
7	1	3	3	3	1	1	1	3	3	3	2	2	2
8	1	3	3	3	2	2	2	1	1	1	3	3	3
9	1	3	3	3	3	3	3	2	2	2	1	1	1
10	2	1	2	3	1	2	3	1	2	3	1	2	3
11	2	1	2	3	2	3	1	2	3	1	2	3	1
12	2	1	2	3	3	1	2	3	1	2	3	1	2
13	2	2	3	1	1	2	3	2	3	1	3	1	2
14	2	2	3	1	2	3	1	3	1	2	1	2	3
15	2	2	3	1	3	1	2	1	2	3	2	3	1
16	2	3	1	2	1	2	3	3	1	2	2	3	1
17	2	3	1	2	2	3	1	1	2	3	3	1	2
18	2	3	1	2	3	1	2	2	3	1	1	2	3
19	3	1	3	2	1	3	2	1	3	2	1	3	2
20	3	1	3	2	2	1	3	2	1	3	2	1	3
21	3	1	3	2	3	2	1	3	2	1	3	2	1
22	3	2	1	3	1	3	2	2	1	3	3	2	1
23	3	2	1	3	2	1	3	3	2	1	1	3	2
24	3	2	1	3	3	2	1	1	3	2	2	1	3
25	3	3	2	1	1	3	2	3	2	1	2	1	3
26	3	3	2	1	2	1	3	1	3	2	3	2	1
27	3	3	2	1	3	2	1	2	1	3	1	3	2

Table 3 Part depth values and S/N ratios

Trial no.	Part depth (mm)		S/N ratio
	*N*1	*N*2	
1	15.50	15.50	20.80
2	15.10	15.00	20.54
3	13.20	13.20	19.40
4	14.20	14.20	20.04
5	14.45	14.45	20.19
6	15.60	15.20	20.74
7	13.80	13.80	19.79
8	15.00	15.00	20.51
9	14.70	14.20	20.18
10	14.80	14.70	20.37
11	14.60	15.40	20.50
12	19.25	20.60	22.96
13	13.40	13.40	19.53
14	15.80	15.60	20.91
15	16.60	16.80	21.44
16	16.20	16.20	21.18
17	15.10	14.30	20.33
18	13.20	12.40	19.12
19	13.80	13.80	19.79
20	20.45	21.65	23.44
21	18.20	21.80	22.90
22	17.00	16.70	21.52
23	15.00	15.40	20.62
24	14.60	14.70	20.31
25	13.40	13.10	19.43
26	15.00	14.80	20.45
27	17.40	17.20	21.75

FEA matched well with the experimentally constructed curves at three different warm-forming temperature levels. Increased limiting strain levels at elevated temperatures were observed. Part depth values from FEA simulations were also compared with the experiments at various die-punch temperature combinations. As showed in Fig. 4, the maximum differences between the FEA predictions and experimental findings were 8% and 10% when the die temperatures were 300°C and 350°C, respectively. A slightly larger discrepancy was observed, however, when T_{die}=200°C and T_{die}-T_{punch}=250-200°C. The errors were in the range of 25-28% in the former case and 23% in the latter case. Less than 8% error, however, was observed in other temperature combinations. Accurate results, however, could be obtained at the expense of costly and lengthy simulations. It took about 30 h to complete one simulation with Dell OptiPlex 755 (Dual 3.0 GHz, 4 GB RAM).

Possible reasons for the discrepancy could be (a) incorrect assumption of contact conditions between tooling and blank. Friction and heat transfer coefficient were assumed uniform and determined based on the information found in the literature and preliminary studies on strain distribution. For more reliable results, these factors need to be determined as a function of temperature and contact pressure; (b) incomplete material modeling. There exists a limitation in obtaining a complete and accurate stress-strain relationship (i.e., flow stress) from tensile tests due to the limitation in the achievable amount of strain when compared to the actual forming process; (c) failure criterion used in simulations. In this study, failure was detected based on the localized necking. However, there is a limitation in predicting material behavior at the limiting strain level, due to insufficient material information. In addition, in an actual forming process, wrinkling and surface defects such as orange peel and Luders lines are

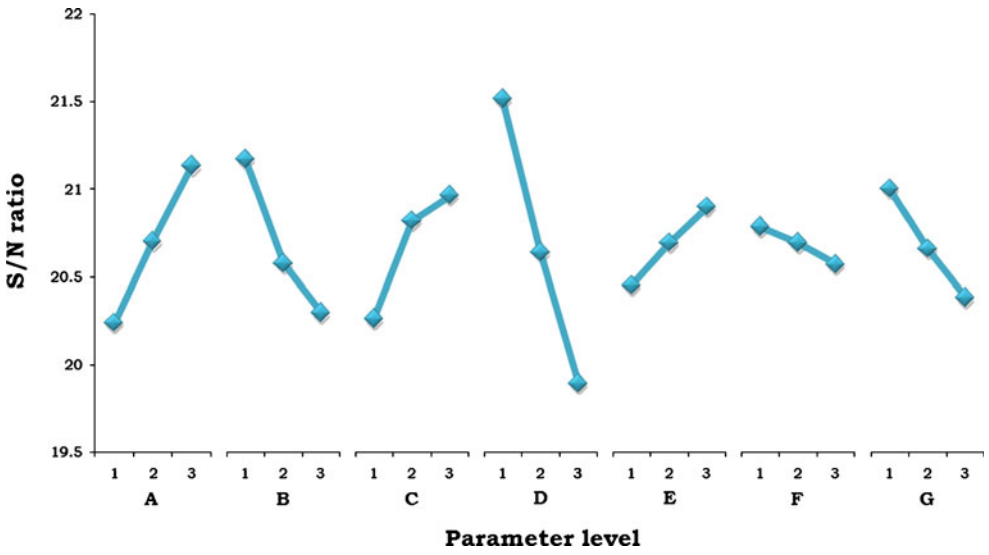

Fig. 5 Main effect of process parameters

also considered to be a failure; (d) possible errors in reporting of experimental results.

3 Combined FEA/DOE using Taguchi method

Taguchi methodology [24] was initially developed in the context of quality engineering. It defines the quality of a product, in terms of the loss imparted by the product to the society from the time the product is shipped to the customer. Part of the success and appeal of Taguchi methodology are that it is general enough to be applied to a wide range of problems that seemingly have very little with quality engineering. It also does not draw upon complicated probability or statistical analysis and generally reduces required number of experiments or simulations by systematically generating the balanced experiment/simulation design. Upon verification of the accuracy and effectiveness of the FEA in predicting material flow and forming limits in warm-forming conditions, Taguchi methodology was used in combination with the FEA to determine a proper combination of warm-forming parameters to achieve high formability. The majors steps required are (1) establishment of objective function, (2) identification of control and noise factors and their levels, (3) selection of an appropriate orthogonal array, (4) trials, (5) analysis of the data and determination of the optimal level, and (6) confirmation.

3.1 Objective and quality characteristic

A performance criterion that reflects how well the warm-forming system is performing needs to be established. For our task, the objective is to determine the optimal combination of process parameters in warm forming which maximize the achievable part depth of a rectangular cup part.

3.2 Control and noise factors

In Taguchi methodology, all factors affecting the process quality can be divided into two types: control factors and noise factors. In general, control factors are easily adjustable by manufacturers and are most important in determining the quality of product characteristics. As many factors as possible should be included so that it would be possible to identify non-significant variables at the earliest opportunity. For the warm-forming case, temperatures of lower die (factor A), punch (factor B) and upper die (factor C), frictions between dies and blank (factor D) and between punch and blank (factor E), punch speed (factor F), and blanking holding pressure (factor G) were selected as control factors and three levels were assigned to each factor as shown in Table 1. All the factors and levels were chosen based on the author's previous research activity [23] and empirical experience.

Noise factors, on the other hand, are difficult or expensive to control and usually exist in the environment (i.e., ambient temperature, humidity, and etc.) causing

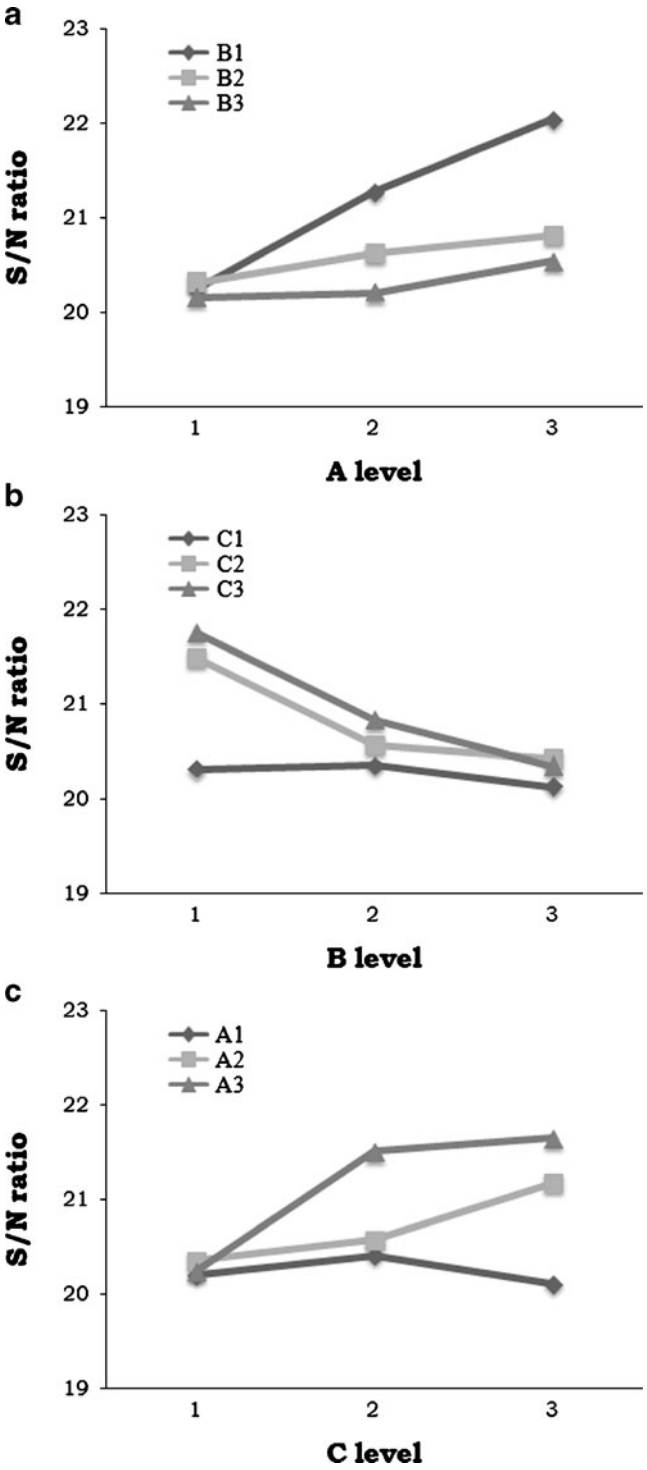

Fig. 6 Interaction effects **a** interaction A×B, **b** interaction B×C, **c** interaction C×A

Table 4 Pareto ANOVA analysis

	Factor and Interaction												
	D	B	A	C	C×A	G	A×B	B×C	E	A×B	B×C	F	C×A
Sum at factor level													
1	193.811	190.704	182.180	182.437	188.668	189.170	183.817	183.722	184.162	184.256	184.728	187.170	187.316
2	185.856	185.294	186.340	187.496	187.277	186.048	186.426	187.374	186.355	187.724	186.629	186.337	185.507
3	179.077	182.745	190.223	188.811	182.798	183.525	188.501	187.647	188.226	186.764	187.387	185.236	185.921
Sum of squares of difference	326.306	99.118	97.062	67.958	56.444	47.992	33.051	28.819	24.821	19.242	11.261	5.649	5.392
Contribution ratio(%)	39.643	12.042	11.792	8.256	6.857	5.831	4.015	3.501	3.016	2.338	1.368	0.686	0.655
Pareto diagram	39.643	12.042	11.792	8.256	6.857	5.831	4.015	3.501	3.016	2.338	1.368	0.686	0.655
Cumulative contribution(%)	39.643	51.685	63.477	71.733	78.590	84.421	88.436	91.937	94.953	97.290	98.659	99.345	100.000
Optimum combination of significant factor levels	$A_3B_1C_3D_1E_3F_1G_1$												

variations in the output. In this warm-forming case, blank temperature distribution before forming was selected as a noise factor, since it changes spatially and temporally depending on the heat transfer rate from the tooling and interface condition. In the first process condition denoted as N1, blank temperature was initially 25°C and forming started as soon as a rectangular blank was clamped between the dies. In the second condition of N2, a rectangular blank was heated between the dies and the punch was moved down after the thermal equilibrium state was reached.

3.3 Orthogonal array

An orthogonal array is the basis for designing experiments or simulations in Taguchi methodology. It provides the shortest possible matrix of combinations in which all the parameters are varied to consider their direct effect as well as interactions simultaneously. In the present investigation, an L_{27} orthogonal array, which has 27 rows corresponding to the number of tests with 13 columns at three levels, was chosen. As shown in Table 2, controllable factors of A-G were assigned to the first, second, fifth, ninth, tenth, 12th, and 13th column, respectively, and the remaining columns were assigned to the two-way interactions of first three factors. Two thousand one hundred eighty-seven ($=3^7$) trials required for a three-level full factorial design with seven factors can be greatly reduced down to 27 trials by using the L_{27} orthogonal array.

3.4 Trials

According to the design matrix in Table 2, non-isothermal FEA runs were performed and part depth values at the failure instance were measured. Signal-to-noise(S/N) ratio was used as the performance index to evaluate the impact of the design parameters on the output quality. Taguchi has empirically found that the two-stage optimization involving S/N ratios indeed gives the parameter level combination, where the standard deviation is minimum while keeping the mean on target [24]. The S/N ratio characteristics can be divided into three categories when the characteristic is continuous:

smaller the better characteristic:

$$S/N = -10\log\left(\frac{1}{n}\sum_{i=1}^{n} y_i^2\right) \tag{1}$$

larger the better characteristic:

$$S/N = -10\log\left(\frac{1}{n}\sum_{i=1}^{n} 1/y_i^2\right) \tag{2}$$

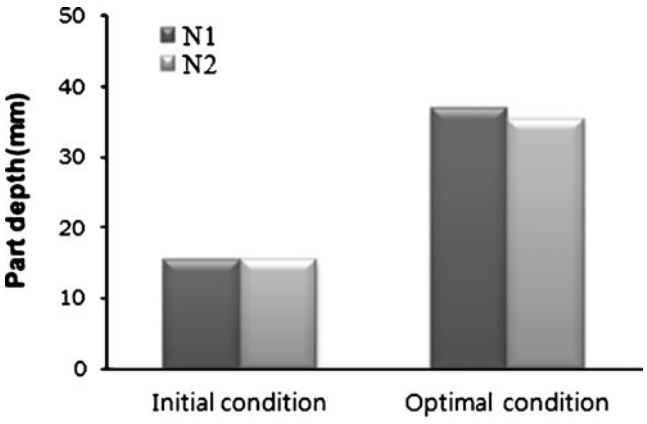

Fig. 7 Part depth values at initial and optimal process conditions

Table 5 Process conditions to evaluate the effects of major process parameters on warm-forming performance

Process parameter	Case	Controllable factors						
		A (°C)	B (°C)	C (°C)	*D*	*E*	*F* (mm/s)	*G* (MPa)
Temperature	Case 1	25	25	25	0.05	0.2	5	1
	Case 2	350	25	350	0.05	0.2	5	1
Friction	Case 3	350	25	350	0.05	0.05	5	1
	Case 4	350	25	350	0.2	0.2	5	1
Punch speed	Case 5	350	25	350	0.1	0.1	5	1
	Case 6	350	25	350	0.1	0.1	20	1
Blank holding pressure	Case 7	350	25	350	0.1	0.1	10	1
	Case 8	350	25	350	0.1	0.1	10	4

nominal is the best characteristic:

$$S/N = 10 \log \frac{\overline{y}}{s_y^2} \tag{3}$$

where y_i is the observed data, n the number of observations, $\overline{y}$ the average of observed data, and s_y^2 the variance of y_i. For each type of characteristic, high value of S/N ratio implies that the signal is much higher than the random effects of the noise factors.

In the present investigation, the objective is to maximize the achievable part depth value, therefore "larger is better" quality characteristics is selected. Table 3 shows the results for part depth and the corresponding S/N ratio.

3.5 Data analysis

Taguchi recommends analyzing the means and S/N ratio using conceptual approach that involves graphing the effects and visually identifying the factors that appear to be significant. Hence, Taguchi's method allows a quick and robust comparison between the factors used in this investigation without analysis of variance (ANOVA) [25] which compares the factors and their interactions via more mathematically tedious calculations. The calculation for determining the effect of a factor was performed by selecting all values of the S/N ratios at each factor level, taking the sum, and dividing by the number of values at each level. The absolute difference between the three averages is the effect of a factor (or interaction). As summarized and plotted in Fig. 5, since a parameter for which the line has the highest inclination has the most significant effect, friction between dies and blank (factor D) has the greatest effect on the achievable part depth value, and next are temperature of the lower die (factor A), temperature of the punch (factor B), and temperature of the upper die (factor C). A lower friction coefficient between dies and blank (i.e., μ=0.05) is recommended to achieve higher formability. In addition, higher temperatures of the dies (i.e., 350°C) and lower temperature of the punch (i.e., 25°C) seems to be favorable to improve formability. Although a friction coefficient between punch and blank (factor E), punch speed (factor F), and blanking holding pressure (factor G) have relatively minor effects on the formability as illustrated in Fig. 5, a higher friction coefficient between punch and blank (i.e., μ=0.2), lower punch speed (i.e. 5 mm/s), and lower blanking holding pressure (i.e. 1 MPa) are the optimal values for improved formability.

When interaction effects were analyzed as shown in Fig. 6, the best combinations for the highest S/N ratios were A×B=350°C×25°C (Fig. 6a), B×C=25°C×350°C (Fig. 6b) and C×A=350°C×350°C (Fig. 6c). Hence, optimal levels of factors A, B, and C acquired from the main effect plot (i.e., Fig. 5) can be recommended again.

One of the methods to analyze data for process optimization is the use of Pareto ANOVA [26], which is a quick and easy method to analyze results of parameter designs. As illustrated in Table 4, it requires least knowledge about ANOVA method and suitable for engineers and industrial practitioners. It is noted that the contribution ratio of friction between dies and blank (factor D), temperature

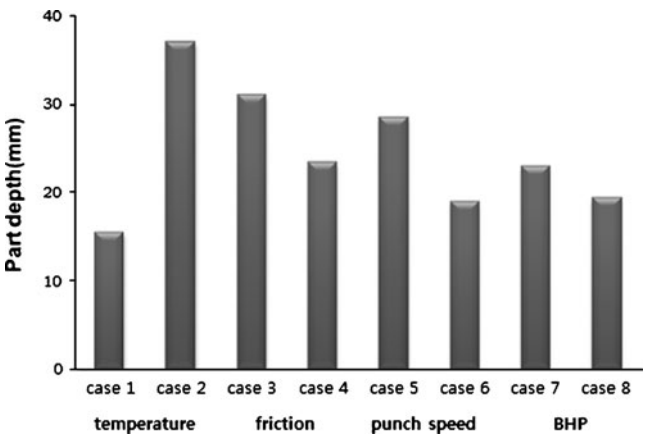

Fig. 8 Forming performance at various temperature, friction, punch speed, and BHP conditions

of the lower die (factor A), temperature of the punch (factor B), and temperature of the upper die (factor C) was more than 70%. The recommended levels of process parameters were the same with the result from Fig. 5.

After the optimal level of process parameters was obtained, a confirmation trial was performed to examine the result of analysis. As shown in Fig. 7, significant increase in part depth value was observed in the optimal process condition (i.e., $A_3B_1C_3D_1E_3F_1G_1$). The part failed at a depth of 37 mm when forming started at T_{blank}=25°C (i.e., N1 case) and slight decrease in depth, 35.2 mm, was observed when punch moved after the thermal equilibrium state (i.e., N2 case). When compared to the initial forming case (i.e., $A_1B_1C_1D_1E_1F_1G_1$) where the part failed at a depth of 15.0 mm, more than 130% increase in part depth can be achieved with a well-controlled warm-forming parameters.

The reliability of the obtained result can be further verified qualitatively through the comparisons with the experimental findings in the literature. In warm forming, usually blank, blank holder, and die are heated up to 200-350°C depending on the alloy type, composition, thickness and part to be formed. However, punch is not usually heated [12, 13]. On the contrary, it is suggested to cool it to keep the temperature at a certain level as it would get heated due to the contact with heated blank. Previous investigations have also identified some process parameters such as punch speed (v), blank holder pressure (BHP), and lubrication (μ) to be significant factors affecting warm-

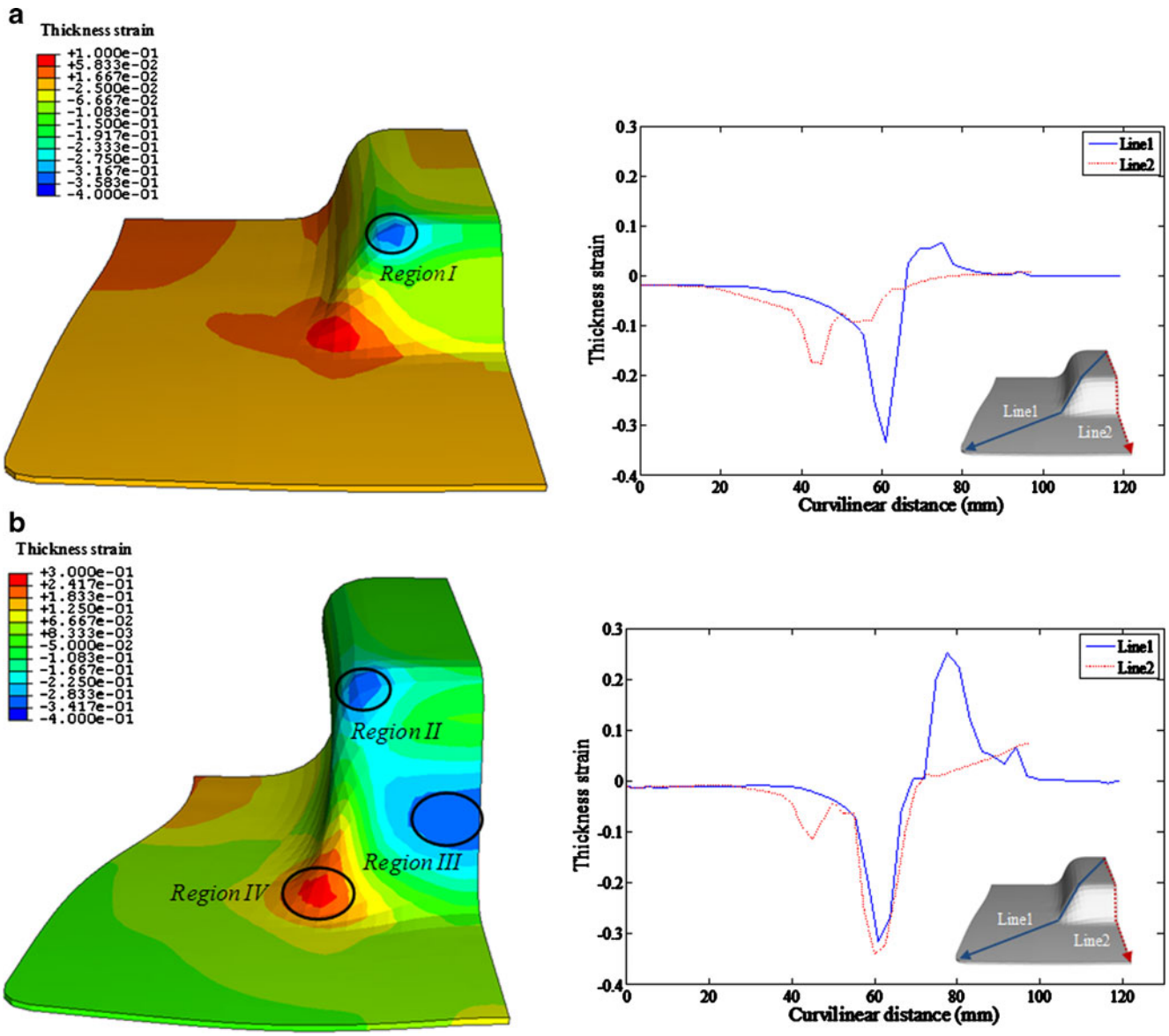

Fig. 9 Thickness strain distribution at two different temperature conditions **a** room temperature (case 1 in Table 5), **b** optimal temperature(case 2 in Table 5)

forming performance. A considerable reduction of formability was observed at a faster forming rate due to increases in flow stress [8, 12]. The initiation of wrinkling was delayed as temperature increases [27]. Hence, a part can be formed with relatively lower BHPs. The friction coefficients of various lubricants between the blank and forming tools were evaluated at warm-forming conditions and lower friction coefficient, in general, was preferable [28, 29].

3.6 Discussion

In order to further expand understandings on the obtained results from the previous section and to evaluate the effects of process parameters on deformation characteristics of the material, strain distributions were investigated at various forming conditions. As shown in Table 5, eight cases were considered with different temperature, friction, punch speed, and blank-holding pressure conditions. The forming performance was summarized in Fig. 8 and the detailed strain distributions at failure were illustrated in Figs. 9, 10, 11, and 12.

Figure 9 shows the thickness strain distributions at two different temperature conditions (i.e., room and optimal temperature conditions). Other process parameters except temperatures were fixed to focus on the pure temperature effect on formability. When the recommended temperatures were realized, the part can be drawn up to a depth of 37 mm as shown in Fig. 9b and considerable amount of strain values were observed in the bottom corner of the part (i.e., region II in Fig. 9b), cup wall region (i.e., region III in

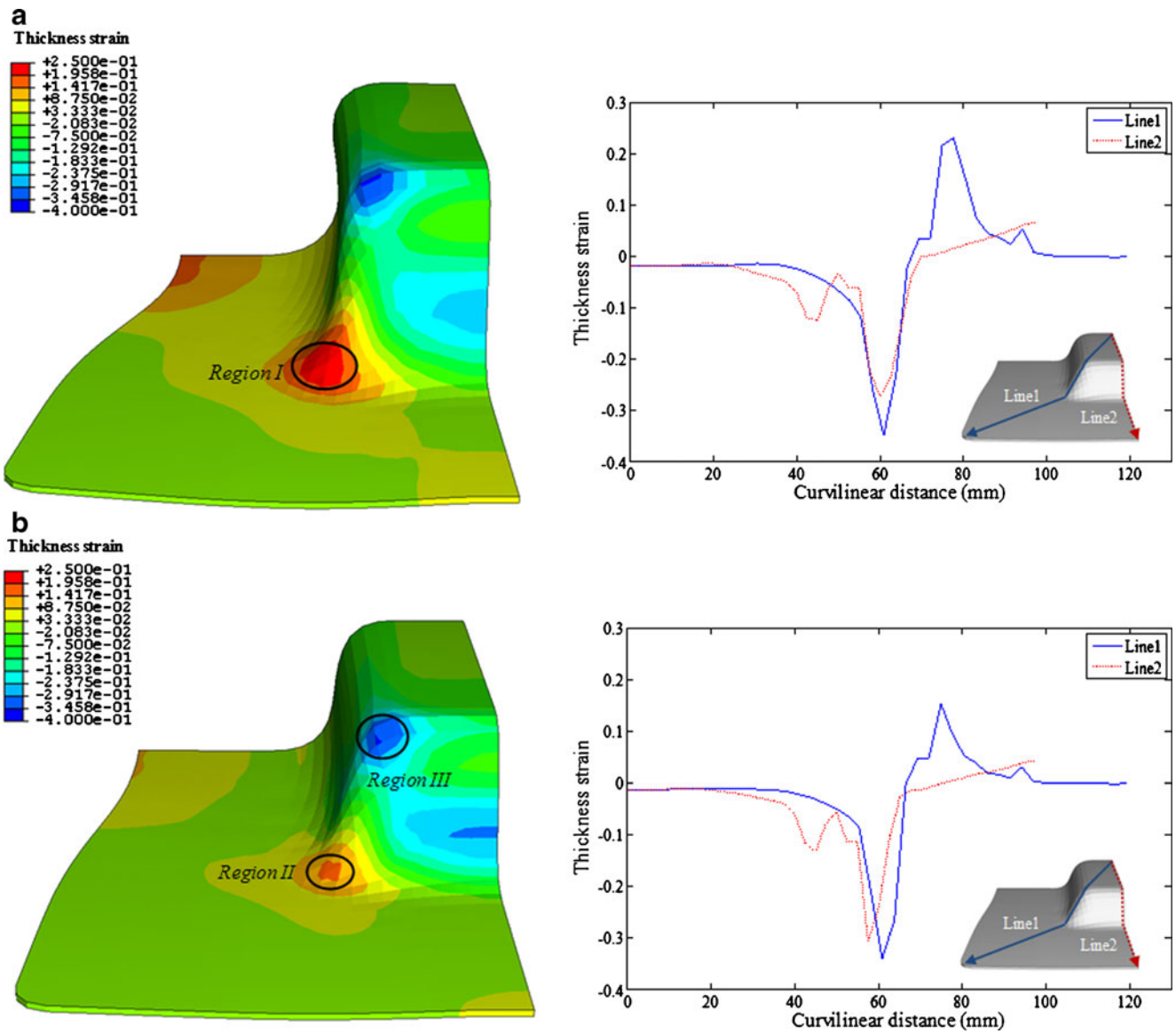

Fig. 10 Thickness strain distribution at two different friction coefficients **a** μ=0.05(case 3 in Table 5), **b** μ=0.2(case 4 in Table 5)

Fig. 9b), and the die corner region (i.e., region IV in Fig. 9b). On the other hand, in the case of room temperature forming (i.e., Fig. 9a), the thinning strain was highly localized around region I and the part failed at a depth of only 15.5 mm. It seems that higher temperatures of the dies increased the ductility of the material in the flange region and allowed more material to be drawn into the die cavity. In addition, lower temperature of the punch increased the flow stress of the blank in the critical failure location and resulted in more uniform thinning and straining characteristic by delaying the localized thinning.

The effect of friction was also analyzed as shown in Fig. 10. In general, lower friction condition was favorable. A much higher part depth value of 31.0 mm was achieved in the case of lower friction coefficient (Fig. 10a), while the failure was observed at a reduced depth of 23.5 mm when the friction coefficient is relatively high (Fig. 10b). In the latter case, it is noted that the deformation of the material in region II was limited when compared to region I in Fig. 10a due to the higher restraining effect of the material in the flange region, and the thinning was highly localized in region III at an early stage of the forming process compared to the former case. It clearly indicates that lower friction condition enables larger plastic deformation of the cup wall region before the onset of the failure by allowing more material flow from the flange region into the die cavity. However, when we compare Fig. 9b with Fig. 10a, a slight increase in formability was obtained in the former case when a higher friction coefficient was assigned between the blank and the punch. Although the overall deformation characteristics in both cases were similar, the magnitudes of thickness strains of the die corner and cup wall regions (i.e.,

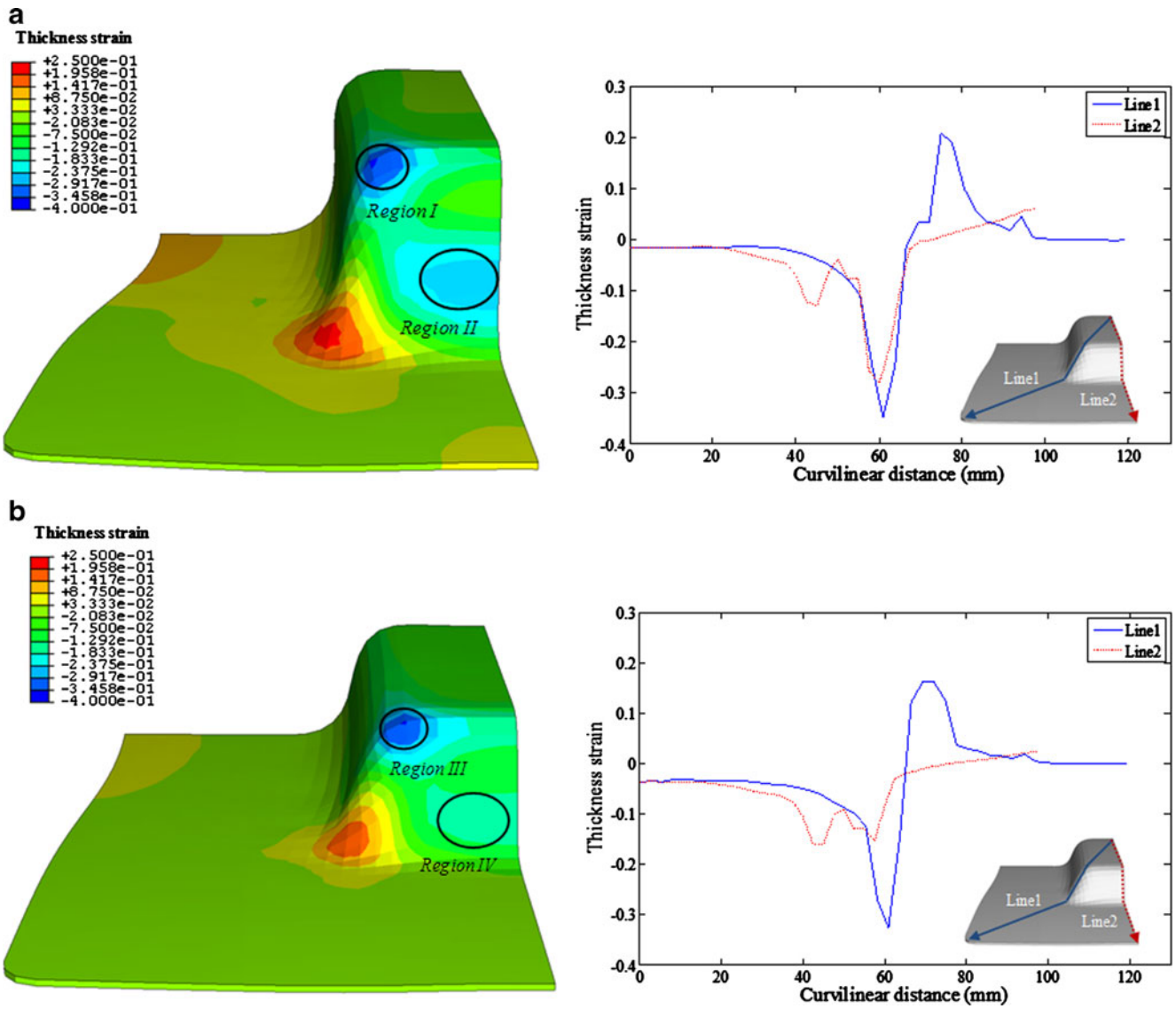

Fig. 11 Thickness strain distribution at two different punch speeds **a** v=5 mm/s (case 5 in Table 5), **b** v=20 mm/s (case 6 in Table 5)

regions III and VI of Fig. 9b) were larger in the case of a higher friction coefficient of the punch. It appears that the increasing friction coefficient between punch and blank enabled the punch force to be transmitted to the blank, and, hence, caused more strain in the die corner region and delayed the thinning initiation. This also agrees with the DOE result of the previous section where higher friction coefficient between punch and blank (factor E) and lower friction coefficient between die and blank (factor D) were recommended for the improved formability. However, when the punch friction coefficient increases beyond a certain level, increasing punch friction is expected to rather accelerate the localized thinning at the failure site due to the increased level of drawing stress in this region. Hence, a careful control of friction depending on the material and process conditions is recommended to maximize the formability.

The effect of punch speed on formability is summarized in Fig. 11. A considerable decrease in part depth was observed with increasing punch speed. In the low punch speed case (Fig. 11a), the critical thinning is detected at a part depth of 28.5 mm, while the part fails at a depth of 19.0 mm when the punch speed is fast (Fig. 11b). In the former case, further decreased flow stress level of the material in the flange region at elevated temperatures and low punch speed seems to enable more uniform plastic deformation of the cup wall region before the failure. Significant deformation of regions I and II in the former case was observed at the failure instant. However, in the latter case, due to the relatively higher flow stress of the material, the deformation of the cup wall (i.e., region IV in Fig. 11b) was greatly reduced when compared to the former case, and, hence, the strain localization is observed at a

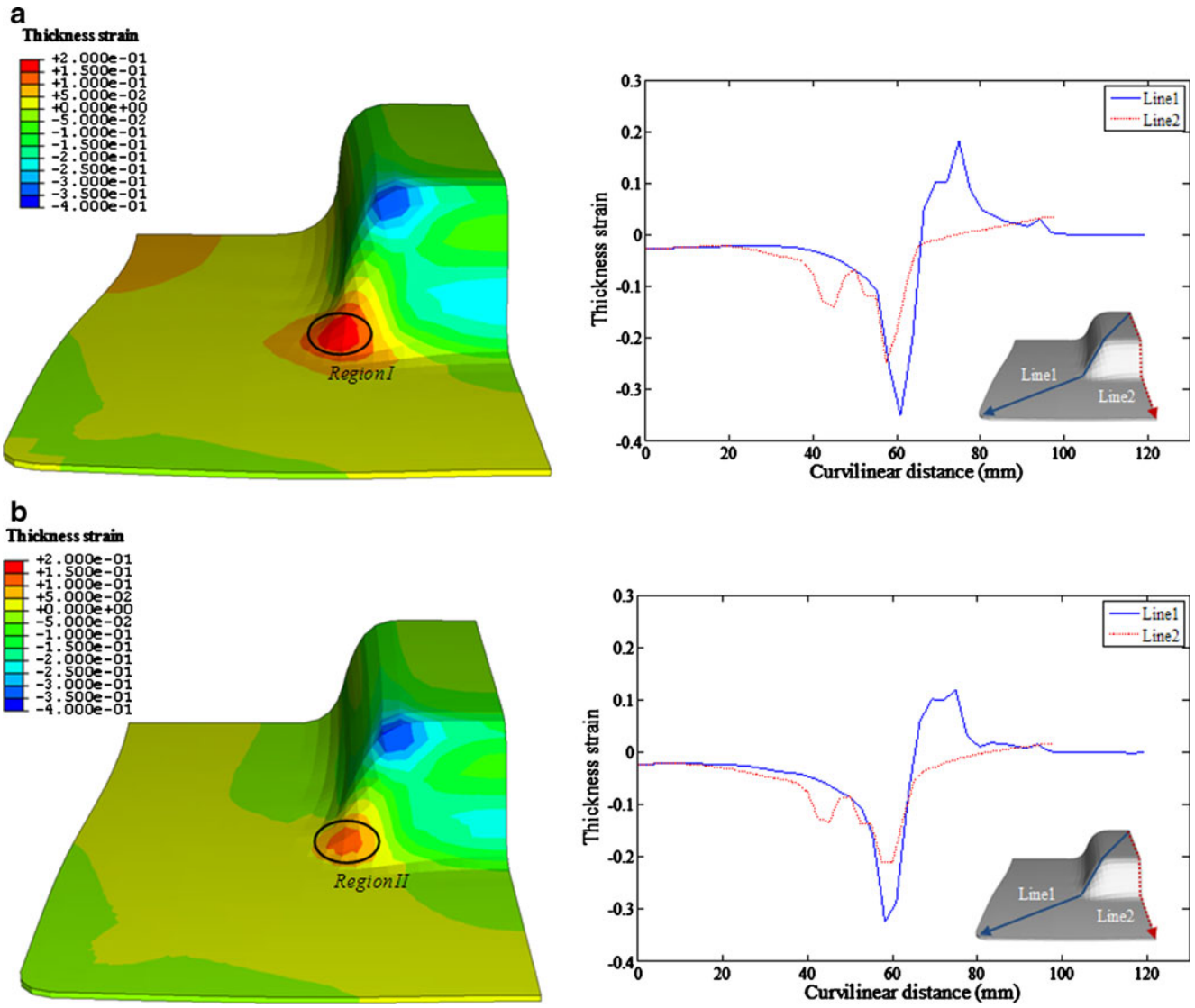

Fig. 12 Thickness strain distribution at two different BHPs **a** 1 MPa (case 7 in Table 5), **b** 4 MPa (case 8 in Table 5)

relatively early stage of the process in the punch corner region (i.e., region III in Fig. 11b). The increased sensitivity of a part depth to forming speed at elevated temperatures agrees with the tensile test results of the material that strain rate sensitivity increases with increasing temperature [10], and slow punch speed is preferred to enhance the formability in warm forming. However, it is recommended that the proper compromise of punch speed should be found for actual warm-forming applications after considering both formability and productivity issues.

Figure 12 shows the effect of BHP on part depth. Lower blank holder pressure is preferred for the improved formability. The achievable part depth values were 23.0 and 19.4 mm in lower and higher BHP cases, respectively. The strain distribution developed showed the similar characteristic in the two cases. However, the magnitude of thickness strains of region I in the lower BHP case (Fig. 12a) was larger than those of region II in the other case (Fig. 12b). Higher BHP seems to prevent the material flow in the flange region and result in the decrease part depth similar to the higher friction forming case. However, beside the localized thinning considered as a failure in this study, wrinkling is another type of failure that frequently occurred in the flange region depending on the BHP level. Therefore, the appropriate level of BHP needs be determined on a part and other process condition basis to obtain the maximum part depth while eliminating the wrinkling.

4 Conclusions

In this study, design of experiments technique in combination with FEA was used to determine the optimal process condition of warm forming with the reduced computational expense. In addition, effects of the major process parameters such as forming temperature, friction condition, punch speed, and blanking holding pressure on forming performance were investigated through an in-depth analysis of strain characteristics at various warm-forming conditions.

(1) The improved formability can be effectively achieved by adopting Taguchi methodology. In the case of rectangular cup forming, appropriate levels of seven major process parameters can be recommended after only 27 trials and significant increase in formability (~130%) can be achieved.
(2) Higher temperatures of the dies and lower temperature of the punch were accepted to achieve much increased formability. The higher temperature level in the flange region increased the ductility of the material and permitted more material to be drawn into the die cavity. The lower temperature level of the die corner increased the flow stress of the blank and delayed the localized thinning in the critical thinning location around the punch corner, resulting in the improved part depth value.
(3) When the punch and the die friction were maintained to the similar level, a monotonic decrease of formability was observed with increasing friction coefficients. However, when the different friction conditions were used for the die and the punch surfaces, higher friction coefficient of the punch surface than the die surface to a certain level enabled to achieve more part depth values due to the improved force transmission from the punch to the blank.
(4) Since the increased restraining force of the material was induced at high BHP, lower BHP is preferred for the increased formability. In addition, the formability showed a considerable decrease with higher punch speed at elevated temperatures due to the increased level of flow stress.

Acknowledgment This research was supported by Basic Science Research Program through the National Research Foundation of Korea (NRF) funded by the Ministry of Education, Science and Technology (2009-0068593).

References

1. Mildenberger U, Khare A (2000) Planning for an environment-friendly car. Technovation 20:205–214
2. Taub A (2000) Automotive materials—technical trends and challenges. Management briefing seminars 2000, Traverse City, MI, USA
3. Berviller L, Bigot R, Martin P (2006) Technological information concerning the integrated design of "net-shape" forged parts. Int J Adv Manuf Technol 31:247–257
4. Vazquez V, Altan T (2000) Die design for flashless forging of complex parts. J Mater Process Technol 98:81–89
5. Dean TA (2000) The net-shape forming of gears. Mater Des 21:271–278
6. Shehata F, Painter MJ, Pearce R (1978) Warm forming of aluminum/magnesium alloy sheet. J Mech Work Technol 2:279–290
7. Li D, Ghosh A (2004) Biaxial warm forming behavior of aluminum sheet alloys. J Mater Process Technol 145:281–293
8. Doege E, Droder K (2001) Sheet metal forming of magnesium wrought alloys—formability and process technology. J Mater Process Technol 115:14–19
9. Takata K, Ohwue T, Saga T, Kikuchi M (2000) Formability of Al-Mg alloys at warm temperatures. Mater Sci Forum 331–337:631–636
10. Li D, Ghosh A (2003) Tensile deformation behavior of aluminum alloys at warm forming temperature. Mater Sci Eng A 352:279–286
11. Ayres RA (1979) Alloying aluminum with magnesium for ductility at warm temperatures (25 to 350°C). Metall Trans A 10:279–290
12. Naka T, Yoshida F (1999) Deep drawability of type 5083 aluminum–magnesium alloy sheet under various conditions of temperature and forming speed. J Mater Process Technol 89(90):19–23
13. Bolt PJ, Lamboo NAPM, Rozier PJCM (2001) Feasibility of warm drawing of aluminum products. J Mater Process Technol 115:118–121
14. Jinta M, Sakai Y, Oyagi M, Yoshizawa S, Matsui K, Noda K (2000) Press forming analysis of aluminum auto body panel:

wrinkle behavior in 5000 and 6000 series aluminum alloy sheet forming. JSAE Rev 21:407–409
15. DOE-USAMP project on warm forming of aluminum. meeting notes and presentations 2002-2003, www.doe.gov/eerl
16. Takuda H, Mori K, Masuda I, Abe Y, Matsuo M (2002) Finite element simulation of warm deep drawing of aluminum alloy sheet when accounting for heat conduction. J Mater Process Technol 120:412–418
17. Palaniswamy H, Ngaile G, Altan T (1999) Finite element simulation of magnesium alloy sheet forming at elevated temperatures. J Mater Process Technol 146:52–60
18. Droder K (1999) Analysis on forming of thin magnesium sheet. University of Hanover, Dissertation
19. Bigot R, Leleu S, Martin P (2003) Forming machine qualification by analysis of manufactured parts geometry: application to aluminium forming process. Int J Adv Manuf Technol 21:476–482
20. Fourment L, Balan T, Chenot JL (1996) Optimal design for non-steady metal forming processes—II. application of shape optimization in forging. Int J Numer Methods Eng 39:51–65
21. Pilani R, Narasimhan K, Maiti SK, Singh UP, Data PP (2000) A hybrid intelligent systems approach for die design in sheet metal forming. Int J Adv Manuf Technol 16:370–375
22. Antonio CAC, Dourado NM (2002) Metal-forming process optimization by inverse evolutionary search. J Mater Process Technol 121:403–413
23. Kim HS, Koç M, Ni J, Ghosh A (2006) Finite element modeling and analysis of warm forming of aluminum alloys-validation through comparisons with experiments and determination of a failure criterion. J Manuf Sci Eng Trans ASME 128:613–621
24. Peace GS (1993) Taguchi methods: a hands-on approach. Addison-Wesley, Reading, MA
25. Schiff D, Dagostino RB (1996) Practical engineering statics. Wiley, Inc
26. Park SH (1996) Robust design and analysis for quality engineering. Chapman and Hall, New York
27. Szacinski AM, Thomson PF (1991) Wrinkling behavior of aluminum sheet during forming at elevated temperature. Mater Sci Technol 7:37–41
28. Sugamata M, Kaneko J, Usagawa H, Suzuki M (1987) Effect of forming temperature on deep drawability of aluminum alloy sheets. Proceedings of the 2nd International Conference on Technology of Plasticity: 1275-1281
29. Naka T, Hino R, Yoshida F (2000) Deep drawability of 5083 Al-Mg alloy sheet at elevated temperature and its prediction. Key Eng Mater 177–180:485–490